Regular Article

PHYSICAL CHEMISTRY RESEARCH
Published by the
Iranian Chemical Society
www.physchemres.org
info@physchemres.org

Phys. Chem. Res., Vol. 12, No. 2, 441-451, June 2024
DOI: 10.22036/pcr.2023.419010.2428

Kinetics of Vinyl Radical with Chlorine Molecules, A Theoretical Study

S.H. Mousavipour[a,b,*] and M. Mehdizade[a]

[a]*Department of Chemistry, College of Science, Shiraz University, Shiraz, Iran*
[b]*Department of Chemistry, Faculty of Science, Sultan Qaboos University, Muscat, Sultanate of Oman*

(Received 2 October 2023, Accepted 4 October 2023)

Different compounds are created when chlorine molecules and vinyl radicals react. Over the lowest doublet potential energy surface, a potential mechanism for this reaction has been put forth at the CBS-QB3 and CCSD(T)/CBSB3 levels of theory. According to theoretical kinetics studies, the dominant product in this system is CH_2Cl-$CHCl$. One deep potential well and 10 distinct channels make up the doublet surface for the reaction in the title. The Single-well multichannel RRKM method along with steady-state approximation for the corresponding intermediate (RRKM-SSA) have been used to estimate the rate constants for the formation of the most likely products that pass through the energized pre-reaction adduct over the temperature and pressure ranges of 300 to 3000 K and 5 to 10,000 Torr. The pressure dependence of various channels is also examined.

Keywords: Vinyl radical, Chlorine molecule, Kinetics, Mechanism, RRKM-SSA

INTRODUCTION

Chlorine has the primary industrial usage in producing a wide range of organochlorine products in developed countries. Chlorinated hydrocarbons are widely used in synthetic polymers, pesticides, and other product manufacturing applications. Some chlorocarbons persist in the environment, which has caused chlorine and chlorinated compounds to become one of the most important environmental pollutants [1,2]. Vinyl radical, the simplest alkenyl radical and crucial component for synthesizing polycyclic aromatic hydrocarbons in acetylene-rich conditions, is one of the chemicals reacting quickly with chlorine [3-5]. The main product, vinyl chloride, causes significant pollution in water, air, food, and, generally, the environment. These chlorinated compounds serve as a crucial source of illnesses and poisonings [6-8].

Numerous studies have been conducted on the role of chlorine atoms and chlorinated compounds in atmospheric processes and their impact on human health. There has been some research done on the generation of hazardous compounds when chlorine reacts with vinyl radicals and unsaturated hydrocarbon free radicals (UHFRs) [9,10].

Well-known two-step chain reactions are a part of the processes governing the gas-phase reactions of hydrocarbon free radicals (R) with chlorine [4,10,11].

The mechanisms of gas-phase reactions of hydrocarbon free radicals (R) with chlorine involve well-known two-step chain reactions [4,10,11].

$$Cl\cdot + RH \rightarrow HCl + R\cdot \qquad (R')$$

$$R\cdot + Cl_2 \rightarrow RCl + Cl\cdot \qquad (R'')$$

Though there is a wealth of knowledge on the interactions of chlorine atoms with saturated hydrocarbons, the reactions of UHFRs with molecular chlorine are only partially understood. Consequently, there are few reported rate coefficient data for the reaction of chlorine with UHFRs (for instance see reference [12] and referenced therein).

Timonen *et al.* [11] used a photoionization mass spectrometer detector to examine the kinetics of reactions

*Corresponding author. E-mail: mousavipour@shirazu.ac.ir

involving vinyl, allyl, and propargyl radicals and Cl2 in a tubular reactor. The following rate constant expression has been reported: $k(C_2H_3 + Cl_2) = 5.24 \times 10^9 \exp(-2.0$ kJ $mol^{-1}/RT)$ M^{-1} s^{-1} in the range of 298 to 435 K. Later, Eskola and Timonen, [4] in a literature review, proposed a rate constant expression for R'' reaction as; $k(C_2H_3 + Cl_2) = (2.79 \pm 0.59)10^9 \exp(3.1 \pm 0.3$ kJ $mol^{-1}/RT)$ l mol^{-1} s^{-1} with a positive activation energy in the range of 200 to 362 K. Although, the kinetics of polyvinyl chloride has been investigated in some extent[13] (because of its significant role in many industries), the kinetics of vinyl chloride seems was not considered as expected. In order to clarify the mechanism of this complex reaction, the current work describes a theoretical investigation of the mechanism of the title reaction on its lowest doublet potential energy surface. According to our research, this system contains a single deep potential well that is essential to the kinetics of the named reaction.

The RRKM approach in conjunction with the steady-state approximation for the active intermediate (RRKM-SSA) [14] was used to observe the effects of the energetic adduct on the dynamics of the title reaction in this single-well multichannel system. For various channels, the concurrent thermal rate constants have been calculated. This method has the advantage of figuring out each channel's rate constant while the other channels are competing. The estimated rate constants are presented for a wide range of pressure (5 to 10,000 Torr) and temperature (300 to 3000 K).

COMPUTATIONAL METHODS

Quantum Mechanical Calculations

To obtain the optimal structures and energies for the stationary points, a composite approach utilizing the full basis set CBS-QB3 [15] was used for structural computations. The five-step CBS-QB3 set of calculations for the geometry optimization at this level of theory is followed by frequency calculations to ascertain thermal adjustments, zero-point vibrational energies, and entropic data. The following three steps include single-point computations on optimized structures at the CCSD(T), MP4SDQ, and MP2 levels. The final energies are provided via the CBS-QB3 extrapolation. At the CCSD(T)/CBSB3 level of theory, the optimized structures' energies were recalculated [16]. In Fig. 1, the proposed PES is displayed. For the relevant zero-

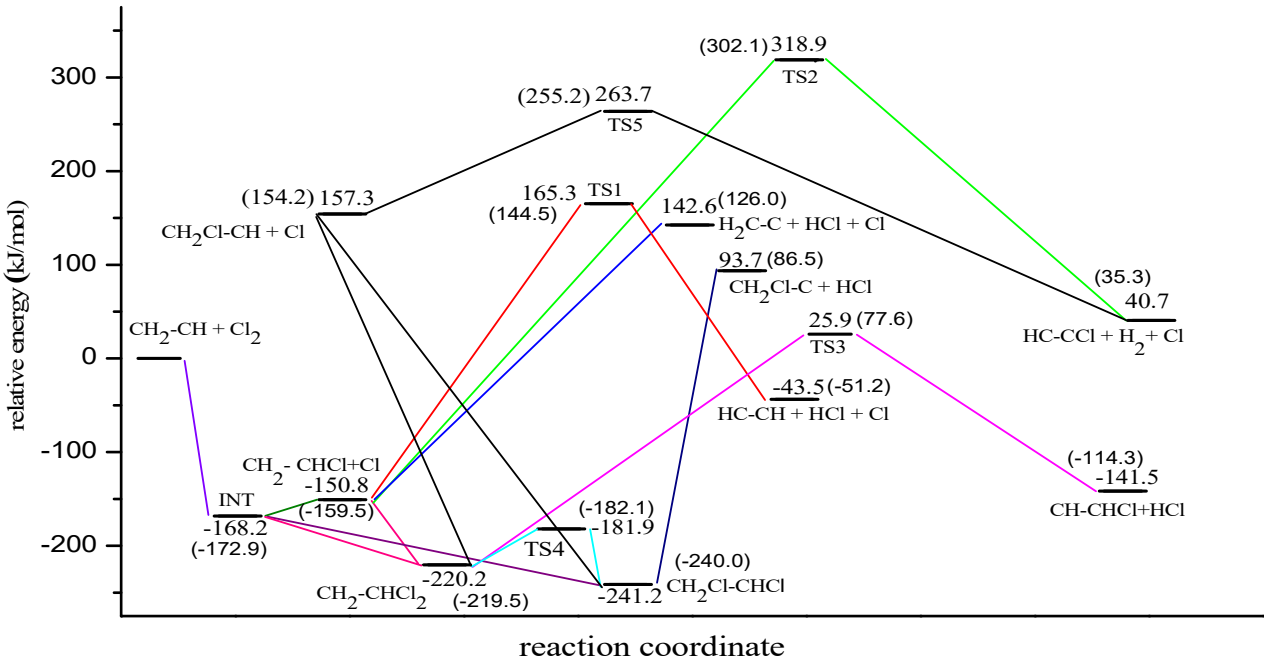

Fig. 1. The global potential energy surface at the CBS-QB3 and CCSD(T)/CBSB3 (in parentheses) levels for the reaction of CH_2=CH with Cl_2. The relative energies are adjusted for the zero-point energies.

point energies (ZPE), all energies are adjusted. To identify the stationary points as first-order saddle points or local minima, we looked at the harmonic vibrational frequencies of each stationary point. In our computations, harmonic frequencies are scaled by a factor of 0.99. To get more precise individual PESs and to investigate the relationships between each saddle point and the related minima along the reaction coordinates, the intrinsic reaction path coordinate [IRCMax(CBS-QB3/B3LYP)] calculations were carried out. In the Supplementary Information file, IRC charts for channels with saddle points are displayed, Figs. S1 to S5. The proposed mechanism is depicted in Scheme 1. The optimized geometries of each stationary point in this system are displayed in Fig. 2. In the Supplementary Information file, the structural z-matrices for the stationary points are provided. Table 1 contains the vibrational term values and moments of inertia for each stationary point.

RESULTS

Potential Energy Surface and Reaction Mechanism

The PES for the title reaction at the CBS-QB3 and

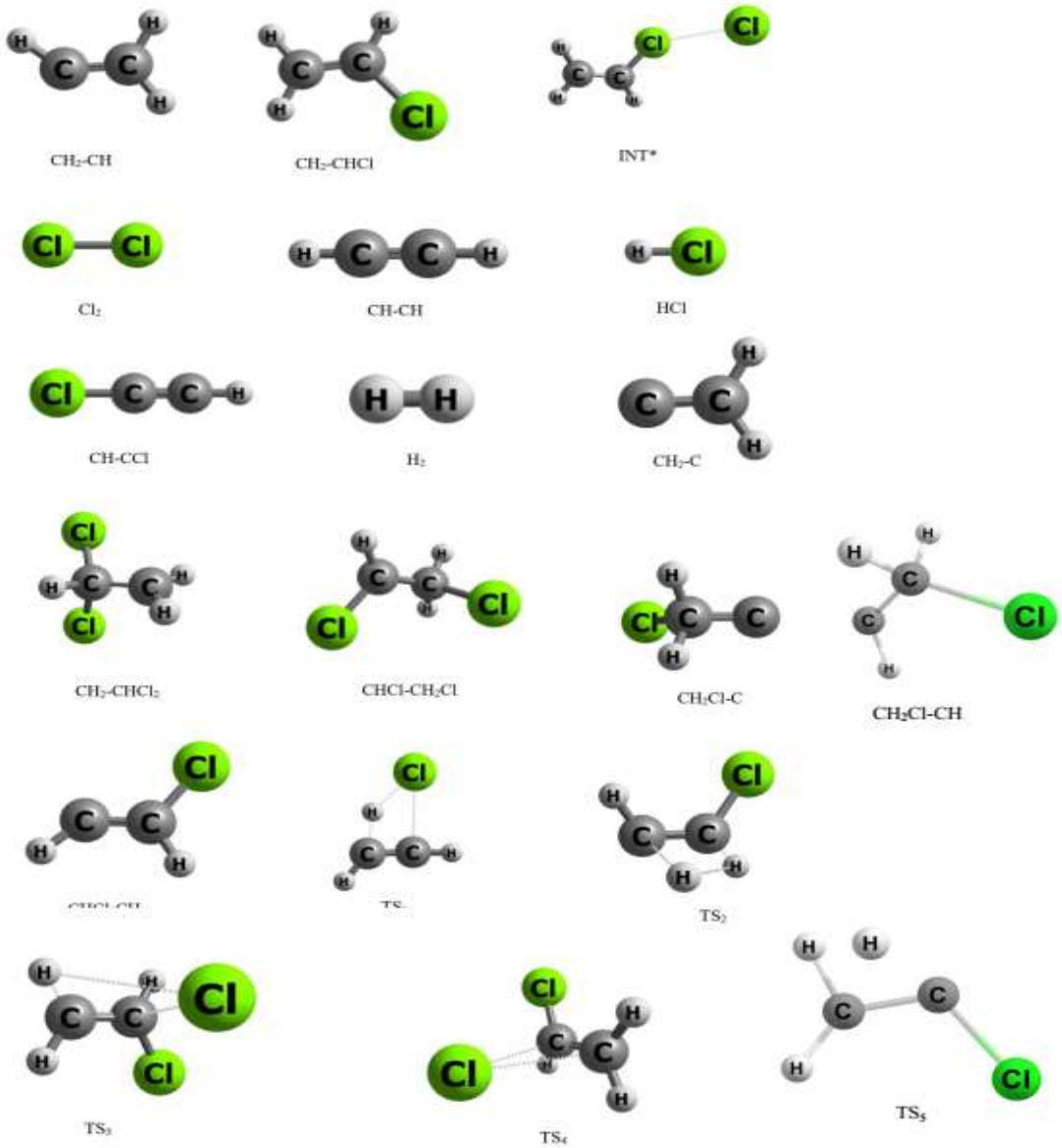

Fig. 2. Optimized stationary points geometries at the B3LYP/CBSB7 level.

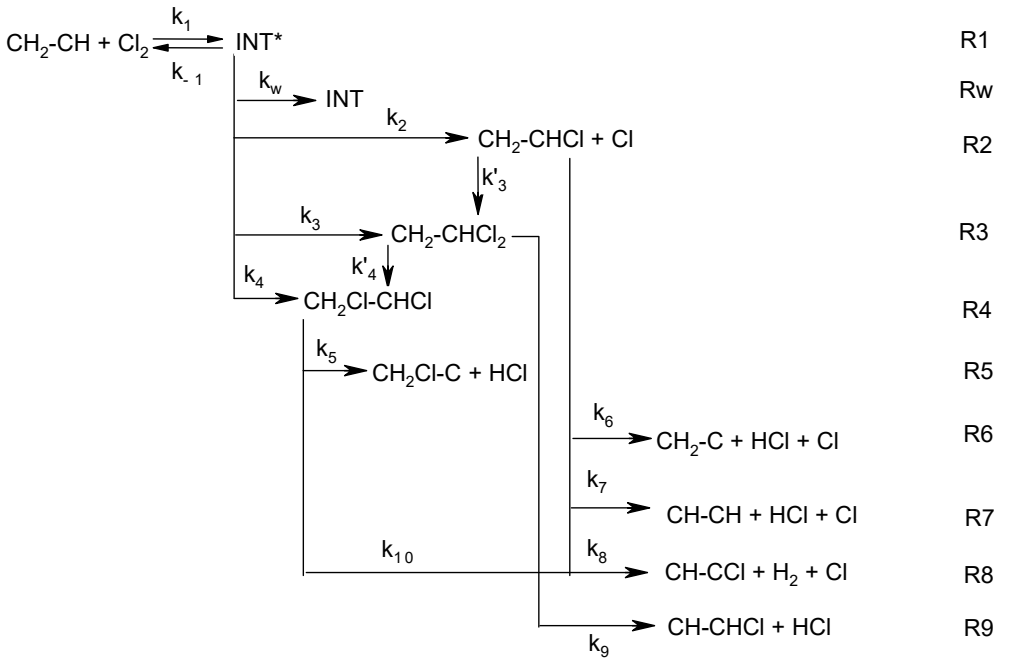

Scheme 1. proposed mechanism for the reaction between the chlorine molecule and the vinyl radical

Table 1. Calculated at the B3LYP/CBSB7 Level are the Stationary Points' Vibrational Term Values and Moments of Inertia. The Scaling Factor for Vibrational Term Values was 0.99

Species	Term values (cm^{-1})	I_i (amu Å^2)
CH_2-CH	3230, 3131, 3041, 1651, 1391, 1047, 922, 821, 715	17.6, 15.5, 2.1
Cl_2	533	72.6, 72.6
INT	3249, 3223, 3152, 1643, 1400, 1300, 1036, 967, 950, 686, 628, 398, 158, 70, 46	311.8, 270.2, 59.6
CH_2-CHCl	3242, 3209, 3148, 1666, 1403, 1303, 1040, 977, 928, 699, 635, 399	94.0, 85.2, 8.8
CH_2-$CHCl_2$	3273, 3162, 3154, 1452, 1299, 1217, 1128, 1002, 667, 623, 537, 397, 291, 262, 149	223.2, 162.1, 74.7
CH_2Cl-CHCl	3221, 3171, 3101, 1470, 1331, 1236, 1177, 1115, 948, 726, 560, 496, 383, 272, 88	285.1, 261.8, 39.5
CH_2Cl-CH	3131, 3117, 3024, 1598, 1332, 1194, 949, 908, 877, 583, 478, 348	102.5, 93.2, 9.4
CH_2Cl-C	3054, 3002, 1314, 1164, 1020, 933, 488, 320, 141	91.9, 84.8, 10.2
CH-CHCl	3147, 2992, 1559, 1162,772, 744, 601, 533, 360.20	89.7, 82.3, 7.42
HCl	2934.67	1.6, 1.6
H_2C-C	3192, 3114, 1709, 1212, 752, 342	14.5, 12.7, 1.8
TS1	3398, 3245, 1779, 1477, 879, 773, 707, 703, 645, 362, 294, 1712i	124.0, 110.0, 14.0
TS2	3245, 3144, 1712, 1290, 972, 941, 724, 655, 599, 422, 399, 1383i	98.6, 92.7, 6.7
TS3	3108, 3091, 1413, 1283, 1169, 932, 800, 680, 642, 574, 434, 383, 111, 1800.01i	253.8, 198.9, 67.0
TS4	3174, 3115, 3054, 1472, 1317, 1213, 994, 896, 876, 702, 536, 379, 221, 188, 241i	252.3, 194.6, 72.6
TS5	3045, 2930, 2097, 1653, 1411, 1099, 937, 725, 588, 339, 188, 1488i	85.6, 85.6, 8.6
HC-CH	3524, 3421, 2070, 773, 751, 642	14.2, 14.2
HC-CCl	3482, 2200, 749, 653, 591, 343	89.3, 89.3
H_2	4419	0.4, 0.4

CCSD(T)/CBSB3 levels of theory is schematically shown in Fig. 1. As would be expected, the dynamics of this system is greatly influenced by the creation of the energetic intermediate INT*. The initial phase (CH_2=CH + Cl_2), according to the ab initio calculations, comprises a barrier-less association reaction that generates the intermediate INT*, which is 172.9 kJ mol^{-1} more stable than the reactants at the CCSD(T) level of theory. The long-range electrostatic interactions between the two anisotropic moieties are crucial in barrier-less association processes. For these types of interactions, many strategies are recommended, for instance, see references [18] and [19]. It has been established that the long-range potential, not the internal dynamics of the complex, should control how a pre-reaction adducts form.

Three possible outcomes for this highly vibrationally energized intermediate following the formation of the activated complex may be assumed: dissociation or isomerization into the other distinct species, stabilization under collisions, or dissociation to return to the reactants. A channel R2 without a saddle point can dissociate this energetic intermediate, INT*, to produce CH_2=CHCl + Cl. The reaction R2 that results in the formation of CH_2=CHCl has three potential unimolecular pathways. By overcoming saddle points TS1 and TS2 with barrier heights of 144.5 kJ mol^{-1} and 302.1 kJ mol^{-1} at the CCSD(T) level, or by forming CH_2=C + HCl (reaction R6) without a saddle point, CH_2=CHCl can undergo a four center dissociation reaction to produce HCCH + HCl (reaction R7) or HCCCl + H2 (reaction R8). Due to the high barrier height present, 144.5 kJ mol^{-1} for TS1, 302.1 kJ mol^{-1} for TS2, and 126.0 kJ mol^{-1} for reaction R6, these routes have little impact on the kinetics of this system. Different products, such as CH_2CHCl_2 (reaction R3) and CH_2Cl- CHCl (reaction R4), are also conceivable from INT* or CH_2=CHCl + Cl. These channels are more stable than the reactants by 219.2 kJ mol^{-1} and 240.0 kJ mol^{-1}, respectively. In reaction R5, which is 86.5 kJ mol^{-1} less stable than the reactants at the CCSD(T), CH_2Cl-CHCl may dissociate into CH_2Cl-C + HCl. In reaction R9, the saddle point TS3 could be passed over by CH_2-$CHCl_2$ with 77.6 kJ mol^{-1} energy at the CCSD(T) level, resulting in CH=CHCl + HCl. Passing over saddle point TS4 to create the primary product in this system (CH_2Cl-CHCl) with 37.4 kJ mol^{-1} activation energy is another route that CH_2-$CHCl_2$ could take. Because of its high energy path (reaction R8) and lack of significance in this system, the formation of CCl-CH from CH_2-CHCl is not important. With a 255.2 kJ mol^{-1} activation energy, the reaction R10, for the formation CH-CCl from CH_2Cl-CHCl followed by CH_2Cl-CH is also not a significant route in this system.

For the standard reaction enthalpy of R2, Timonen *et al.* [11] proposed a value of -147 kJ mol^{-1}, and Lee *et al.* [12] reported a value of -158 kJ mol^{-1} at the CBSQ level of theory. According to our findings, the reaction enthalpy for R2 at the CBS-QB3 level of theory is -153 kJ mol^{-1}.

Rate Constants Calculations

The RRKM-SSA approach [14] was used to determine the rate constants of those channels (reactions R2, R3, R4, and Rw) that are significant in this system and connected directly to the potential well INT* based on the structure of the PES from the CCSD(T) method.

As might be expected, there is uncertainty in finding the location of the bottleneck for barrier-less reactions. As available energy decreases, the bottleneck for the interaction typically occurs at greater distances where the two reacting species are only weakly interacting as a result of getting closer to one another and the sum of states decreasing as a function of available energy in the system.

Within the framework of this procedure, the following equation was employed to compute the microcanonical rate constants [17]:

$$k(E,J) = \sigma N^{\#}(E,J)/h\rho(E,J) \quad (1)$$

Where the state density of the reactant (here INT* for the reverse reaction (R-1)) ($\rho(E,J)$), Planck's constant (h), the sum of the states of the saddle point ($N^{\#}(E,J)$), and reaction path degeneracy (σ) were taken into consideration. The bottleneck for the initial association reaction was located using this microcanonical rate constant estimate. Based on the data gathered from the microcanonical rate constants $k(E, J)$ calculations for each of the distinct reactions, thermal rate constants (k(T)) at various pressures and temperatures were computed.

The energy step size ($\Delta E^{\#}$) for calculating $k(E)$ in RRKM calculations was set to 1.3 kJ mol^{-1} up to 120.0 kJ mol^{-1}. The collision efficiency (βc) value of 0.5 was utilized [18] at lower temperatures and dropped to a value of 0.2 at higher

temperatures. N_2 was used as the bath gas since it is more useful for environmental issues. Using the calculating approach outlined by Loukhovitski and Sharipov [19], a value of 4.28 Å was selected for the collision diameter in a nitrogen bath gas environment.

The transitional modes in reactions involving two separated reactants are those vibrational and rotational degrees of freedom that are specifically relevant to the reaction [20]. The total and density of states over the active vibrational and rotational states were computed using the direct count. For association reactions normally internal rotations are not taken into account. It is presumed that the K-rotational states are active [21,22].

As the two reactants move toward one another to produce the bottleneck, we were unable to locate any saddle points for the entrance channel of R1. The bottleneck for the reverse reaction of R1 (creation of CH_2-CH + Cl_2 from the INT* complex) was calculated *via* microcanonical variational RRKM calculations to range from 3.41 (the C-Cl bond distance) at lower energies (temperatures) to a value of 1.98 at higher energies (temperatures).

Based on a modified version of Zhu and Hase's RRKM program, the steady state approximation (SSA) method was used to the following unimolecular reactions to get the subsequent formulations for the rate constants of bimolecular reactions:

$$k_{bi} = \frac{\sigma B_e Q_a^{\#}}{hQ_A\, Q_B} exp\left(\frac{-E_0}{RT}\right) \Delta E^{\#} \sum_{E_0}^{\infty} \frac{G(E_{vr}^{\#})\, exp(-E^{\neq}/RT)}{1+\frac{k\,(E^*)}{w}} \quad (2)$$

The approach given by Dean [24] (based on RRKM theory in conjunction with the steady-state assumption for the energized intermediates) was used to compute the individual rate constants for reactions R2, R3, R4, and intermediate stabilization kw. Based on this method, the following equations for the second-order rate constants of channels RW, R2, R3, and R4 are obtained. We overlooked the reactions R_3' and R_4' in our calculations.

$$k_w = \frac{\sigma B_e\, Q_a^{\neq}}{h\, Q_{C2H3} Q_{Cl2}}\ exp^{\left(-\frac{E_a}{RT}\right)}\ \sum_{E0}^{\infty} \frac{W\{G(E^+)\}\exp\left(-\frac{E^+}{RT}\right)}{k_4+k_3+k_2+k_{-1}+w} \quad (3)$$

$$k_{bi}(R_2) = \frac{\sigma B_e\, Q_a^{\neq}}{h\, Q_{C2H3} Q_{Cl2}}\ exp^{\left(-\frac{E_a}{RT}\right)}\ \sum_{E0}^{\infty} \frac{K_2(E)\{G(E^+)\}\exp\left(-\frac{E^+}{RT}\right)}{k_4+k_3+k_2+k_{-1}+w} \quad (4)$$

$$k_{bi}(R_3) = \frac{\sigma B_e\, Q_a^{\neq}}{h\, Q_{C2H3} Q_{Cl2}}\ exp^{\left(-\frac{E_a}{RT}\right)}\ \sum_{E0}^{\infty} \frac{K_3(E)\{G(E^+)\}\exp\left(-\frac{E^+}{RT}\right)}{k_4+k_3+k_2+k_{-1}+w} \quad (5)$$

$$k_{bi}(R_4) = \frac{\sigma B_e\, Q_a^{\neq}}{h\, Q_{C2H3} Q_{Cl2}}\ exp^{\left(-\frac{E_a}{RT}\right)}\ \sum_{E0}^{\infty} \frac{K_4(E)\{G(E^+)\}\exp\left(-\frac{E^+}{RT}\right)}{k_4+k_3+k_2+k_{-1}+w} \quad (6)$$

According to Scheme 1, $k_{bi}(R_x)$s are the rate constants for the relevant channels, and k_W is the stabilization rate constant for the energized intermediate INT*. The bottleneck of the initial association reaction is represented by $Q_a^{\#}$, which is the product of the vibrational and rotational partition functions. Q_{C2H3} and Q_{Cl2} are the products of the reactants partition functions. $G(E^+)$ is the sum of the vibrational and rotational states of the corresponding TS at the internal energy E^+. $w\,(=Z\beta_c[A])$ is the collisional stabilization for energized intermediate. As determined by the RRKM approach, which divides the sum of states by the density of states for the corresponding steps, $k_x(E)$s is the microcanonical rate coefficient for the corresponding steps in the energy range of E to $(E+\Delta E)$. The electronic partition functions' ratio, B_e, is determined as

$$B_e = \frac{q_{elec}^{\neq}}{q_{elec,C2H3}\, q_{elec,Cl2}} \quad (7)$$

The pressure-dependent stage of the association reaction that creates the pre-reaction intermediate INT (k_W) is as expected. The pressure-dependent of k_W at 500, 1000, and 2000 K in the pressure range of 5 to 10,000 Torr (0.007 to 13.2 atm) is shown in Fig. 3.

Figures 4 and 5 depict the Arrhenius charts for the rate constants of reactions R_W, R2, R3, and R4 at 760 Torr and 10,000 Torr pressure.

The following formulas were obtained by non-linear least-squares fitting to the computed rate constants at the CCSD(T) level of theory at 760 Torr in Fig. 4:

$k_2 = 8.8 \times 10^{14} \times T^{0.11}$ exp(-15.0 kJ mol^{-1}/RT) l mol^{-1} s^{-1}

$k_3 = 5.3 \times 10^{15} \times T^{0.01}$ exp(-13.5 kJ mol^{-1}/RT) l mol^{-1} s^{-1}

$k_4 = 1.9 \times 10^{16} \times T^{0.01}$ exp(-12.7 kJ mol^{-1}/RT) l mol^{-1} s^{-1}

$k_w = 4.0 \times 10^{15} \times T^{-0.70}$ exp(-11.5 kJ mol^{-1}/RT) l mol^{-1} s^{-1}

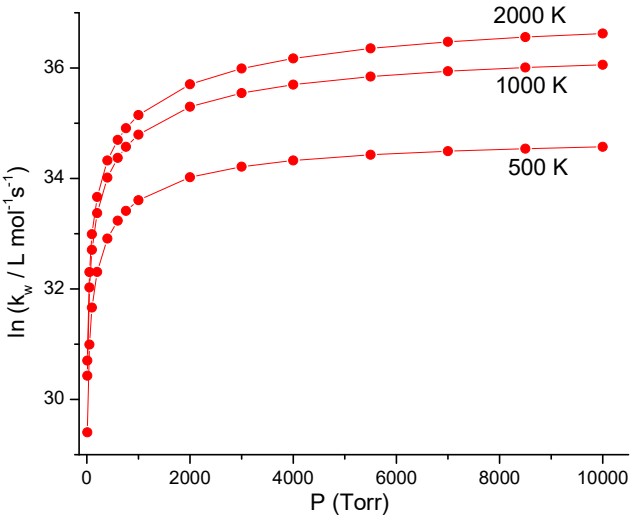

Fig. 3. The intermediate stabilization rate constant k_W changes as a function of pressure and temperature.

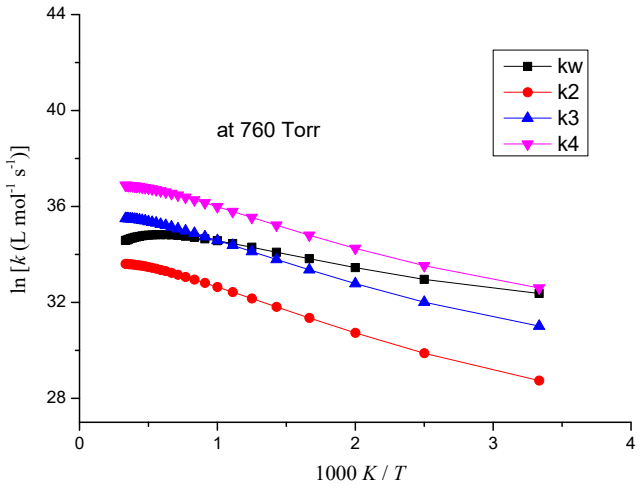

Fig. 4. Shows the calculated Arrhenius plots for reactions R2, R3, R4, and R_W at 760 Torr using the RRKM-SSA technique.

At lower pressures and higher temperatures, reactions R3 and R4 (creation of CH_2-$CHCl_2$ and CH_2Cl-CHCl, respectively) dominate, whereas reaction R2 (production of CH_2-CHCl + Cl) plays a less significant role. As anticipated, at lower temperatures, the stabilization rate constant kw is equivalent to the rate constants for reactions R3 and R4, whereas at higher temperatures, it tends to decrease. Deactivation reaction Rw becomes the main pathway in this system at

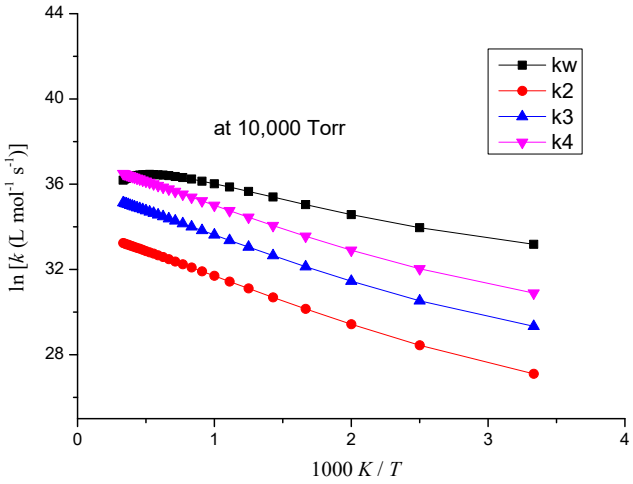

Fig. 5. Arrhenius plots calculated using the RRKM-SSA method for reactions R2, R3, R4, and R_W at 10,000 Torr.

higher pressures (10,000 Torr), as seen in Fig. 5.

The following expressions were obtained at the CCSD(T) level of theory by non-linear least-squares fitting to the data in Fig. 5 at 10,000 Torr:

$$k_2 = 3.5 \times 10^{14} \times T^{0.37} \exp(-15.3 \text{ kJ mol}^{-1}/RT) \text{ l mol}^{-1} \text{ s}^{-1}$$

$$k_3 = 2.0 \times 10^{15} \times T^{0.45} \exp(-13.9 \text{ kJ mol}^{-1}/RT) \text{ l mol}^{-1} \text{ s}^{-1}$$

$$k_4 = 7.4 \times 10^{15} \times T^{0.50} \exp(-13.1 \text{ kJ mol}^{-1}/RT) \text{ l mol}^{-1} \text{ s}^{-1}$$

$$k_w = 2.3 \times 10^{16} \times T^{-0.67} \exp(-13.9 \text{ kJ mol}^{-1}/RT) \text{ l mol}^{-1} \text{ s}^{-1}$$

Channels R2, R3, and R4 showed no discernible pressure dependence across the pressure range of 760 to 10,000 Torr. It should be noted that these four channels are in direct competition, therefore raising one channel's rate will affect the rates of the others.

The system may go through reactions R5 to R10 as depicted in Scheme 1 after the products of reactions R2 to R4 are generated. The unimolecular reactions R5 to R10 are less significant because of their comparatively high activation energies. The density, sum of states, and microcanonical rate constants ($k(E)$) for the respective saddle points and channels were calculated using the RRKM method. Using these data and the circumstances stated for reactions R2 to R4, $k(T)$

values for these channels were calculated. For Reactions R5 and R6, as predicted, no saddle point was revealed. As a result, the microcanonical variational RRKM approach was used to pinpoint the locations of the respective bottlenecks for both processes. At lower temperatures, the positions of the bottlenecks for reactions R5 and R6 were 3.5 Å and 3.7 Å, respectively, and they decreased to 2.1 Å and 2.2 Å at higher temperatures for the C-Cl bonds. Figures 6 and 7 show the Arrhenius plots for the rate constants of reactions R5 to R9 at 760 Torr and 10,000 Torr, respectively. In this system, reaction R10 was not significant.

The following rate expressions at 760 Torr are produced by fitting the data in Fig. 6.

$k_5 = 1.9 \times 10^{17} \times T^{0.78} \times \exp(-33.1 \times 10\ \text{kJ mol}^{-1}/RT)$ l mol^{-1} s^{-1}

$k_6 = 8.1 \times 10^{17} \times T^{0.12} \times \exp(-29.3 \times 10\ \text{kJ mol}^{-1}/RT)$ l mol^{-1} s^{-1}

$k_7 = 2.3 \times 10^{17} \times T^{0.80} \times \exp(-37.4 \times 10\ \text{kJ mol}^{-1}/RT)$ l mol^{-1} s^{-1}

$k_8 = 9.6 \times 10^{17} \times T^{2.11} \times \exp(-47.0 \times 10\ \text{kJ mol}^{-1}/RT)$ l mol^{-1} s^{-1}

$k_9 = 1.9 \times 10^{19} \times T^{1.73} \times \exp(-25.9 \times 10\ \text{kJ mol}^{-1}/RT)$ l mol^{-1} s^{-1}

From 5 to 10,000 Torr, the pressure dependence of reactions R5 through R9 were studied. The tunneling correction may not be so significant for these reactions because their activation energies are larger in comparison to the total energy of the reactants. Using Brown's model [25], which is detailed in reference [14], the tunneling factor (κ) was estimated as a hydrogen atom approaches a one-dimensional unsymmetrical Eckart barrier [26].

The following rate expressions at 10,000 Torr result from the fitting method on the date in Fig. 7.

$k_5 = 1.9 \times 10^{17} \times T^{0.81} \times \exp(-33.1 \times 10\ \text{kJ mol}^{-1}/RT)$ l mol^{-1} s^{-1}

$k_6 = 1.1 \times 10^{18} \times T^{0.70} \times \exp(-29.1 \times 10\ \text{kJ mol}^{-1}/RT)$ l mol^{-1} s^{-1}

$k_7 = 9.4 \times 10^{17} \times T^{1.60} \times \exp(-31.1 \times 10\ \text{kJ mol}^{-1}/RT)$ l mol^{-1} s^{-1}

$k_8 = 1.0 \times 10^{18} \times T^{3.09} \times \exp(-46.8 \times 10\ \text{kJ mol}^{-1}/RT)$ l mol^{-1} s^{-1}

$k_9 = 2.3 \times 10^{19} \times T^{2.64} \times \exp(-25.7 \times 10\ \text{kJ mol}^{-1}/RT)$ l mol^{-1} s^{-1}

DISCUSSION

Our calculations show that the addition of Cl_2 to the vinyl

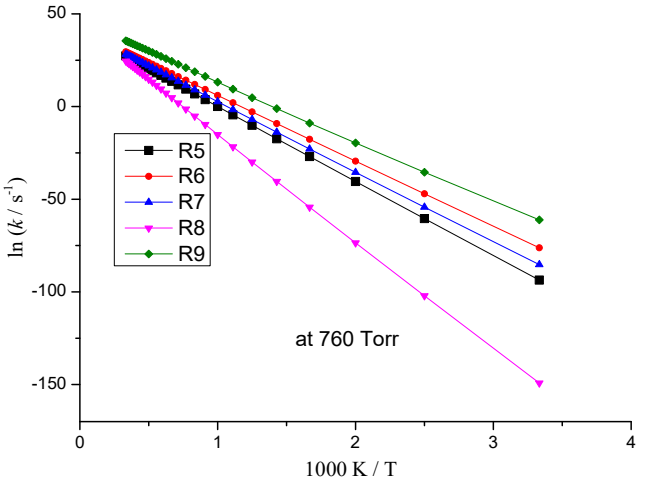

Fig. 6. Arrhenius graphs from RRKM calculations at 760 Torr for channels R5 to R9.

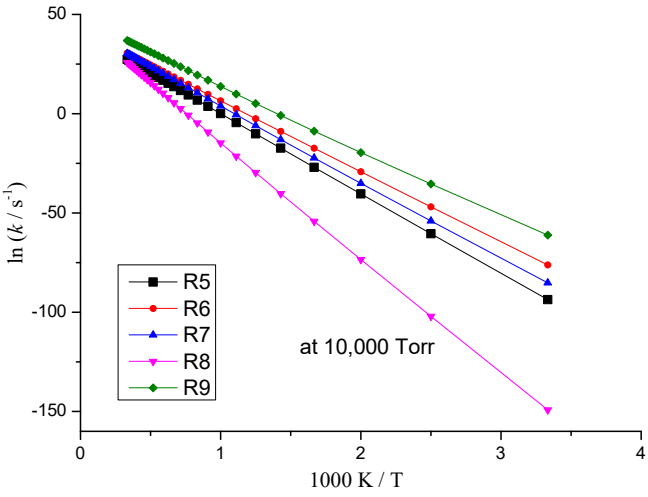

Fig. 7. Arrhenius graphs from RRKM calculations at 10,000 Torr for channels R5 to R9.

radical is a successive process, as one of us stated in reference [27]. Pre-reaction energized adduct INT* with one chlorine atom linked to the C with fewer hydrogen must first be formed before the subsequent reactions that can take place in this system. The barrierless interaction of the hydrocarbon radical with the chlorine molecule is the initial process. As anticipated, the long-range interactions between the two moieties play a major role in the creation of the intermediate INT*. As the INT* is formed, the reactants' external rotations and radial components of relative translations eventually change into vibrations, internal rotations, torsional modes, and tumbling or rocking motions. If the intramolecular vibrational redistribution (IVR) process is not so fast to cause the relaxation of vibrational energy through distribution among the other modes, the newly formed C-Cl bond will immediately dissociate due to its high level of energy. It has been anticipated that the IVR process in this system moves far more quickly than reactive collisions, isomerization, or dissociation. Since we will be working on the dynamics of the title reaction in the near future, it was not planned for the current study to go over the specific dynamics of this system in detail. For highly energetic O-H or O-O bonds, the time scale for IVR is in the order of a picosecond, according to a study from our lab on the dynamics of the H atom reaction with the HO_2 radical [28]. For the newly formed C-Cl bond in this system, it has been assumed a nearly identical IVR time scale, which should be on the same order for the masses of matching moieties [29].

The deactivation rate constant (k_w) at lower temperatures is comparable to the rates of the other three competing channels (R2, R3, and R4), according to Fig. 4 at 760 Torr with low energy over the PES. While k_w does not much change as expected, the rates of channels R3 and R4 increase as the temperature rises in terms of their path energy. As would be expected, as the binding becomes more exothermic at higher temperatures, the value of k_w increases to a maximum value. The deactivation rate constant (k_w) plays a substantial role in comparison to the other competing rate constants R2 to R4 at lower and higher temperatures, as seen in Fig. 5 at 10,000 Torr. As seen in Figs. 4 and 5, the low-lying vibrational states that become significant at higher temperatures are the cause of the rate constants for channels R2, R3, and R4 to curve. Given that the reactants have sufficient internal energy to cross over the respective saddle points, tunneling for these three channels was not crucial. The production of CHCH and CHCCl is not significant in this system due to the high activation energies (TS1 and TS2); instead, reactions R5 to R9 are unimolecular reactions that become significant channels as the temperature rises above 1000 K. Reactions R7, R8, and R9 cross the appropriate saddle points, TS3, TS1, and TS2, as indicated in Scheme 1. In this study, it was assumed that the reactants' energy for reactions R5 to R9 was transferred through collisions and that they were no longer energized. Figure 2 depicts the saddle points' structures. Moments of inertia and vibrational term values for the stationary points are shown in Table 1.

Over the pressure range of 5 to 10,000 Torr, the pressure dependence for all channels was investigated. The association reaction R1 and the unimolecular reactions R5 to R9 are pressure-dependent to some extent, as demonstrated in Fig. 3 and S6 to S15. The position of P1/2 is indicated in Fig. S6 through S15 by (×).

Figures 4 and 5 can be compared, and Fig. 5's rate constants for R2 to R4 are smaller than those in Fig. 4's. At increasing pressures, the competing rate constants R2 to R4 drop as the association rate constant k_w rises. Figures S6 to S15 demonstrate that at lower temperatures, the tunneling factor nearly doubles the rate constants, whereas at higher temperatures, the tunneling process is negligible.

CONCLUSIONS

At the CBS-QB3 and CCSD(T) levels of theory, the mechanism and kinetics of the reaction between vinyl radicals and chlorine molecules over the lowest doublet PES are examined. To the best of our knowledge, the kinetics of this reaction have not been thoroughly studied and published in the literature. For the title reaction, ten different channels are taken into account. With the strong collision assumption, which results in more efficient energy transfer during collisions, the rate constant for each path was estimated using the RRKM-SSA approach. The reaction was examined over the pressure range of 5 to 10,000 Torr in order to investigate the impact of pressure on the creation of the products. We were unable to find any substantial consequences of this pressure dependence on the creation of the other various immediate products, while the pressure clearly had an impact on the rate of stabilization and consumption of the energized

intermediate. At lower pressures, the title reaction's main product was predicted by the RRKM-SSA technique to be CH_2Cl-CHCl, whereas at higher pressures, stabilization of the INT* was projected to be more significant. For reactions Rw and R2 to R9, the computed rate coefficient was presented. The unimolecular reactions R5 to R9 exhibit some pressure dependence. Overall, this study demonstrates the necessity for more thorough experimental and dynamic research to deepen our understanding of systems containing chlorinated hydrocarbons.

ACKNOWLEDGEMENTS

The Research Council of Shiraz University is thanked for their financial assistance.

REFERENCES

[1] Macdonald, R. W.; Morton, B.; Johannessen, S. C., A review of marine environmental contaminant issues in the North Pacific: The dangers and how to identify them. *Environ. Rev.*, **2003**, *11* (2), 103-139, DOI: 10.1139/a03-017.

[2] Huang, B.; Lei, C.; Wei, C.; Zeng, G., Chlorinated volatile organic compounds (Cl-VOCs) in environment-sources, potential human health impacts, and current remediation technologies. *Environ. Int.* **2014**, *71*, 118-13, DOI: 10.1016/j.envint.2014.06.01.

[3] Troe, J., Toward a Quantitative Analysis of Association Reactions in the Atmosphere. *Chem. Rev.* **2003**, *103* (12), 4565-4576, DOI: 10.1021/cr020514b.

[4] Eskola, A. J.; Timonen, R. S., Kinetics of the reactions of vinyl radicals with molecular oxygen and chlorine at temperatures 200-362 K. *Phys. Chem. Chem. Phys.* **2003**, *5* (12), 2557-2561, DOI: 10.1039/B302894A.

[5] Cheeseman, K. H.; Slater, T. F., An introduction to free radical biochemistry. *Br. Med. Bull.: BMB.* **1993**, *49* (3), 481-493, DOI: 10.1093/ oxfordjournals.bmb.a072625.

[6] Al-Malack, M. H.; Sheikheldin, S. H., Effect of solar radiation on the migration of vinyl chloride monomer from unplasticized PVC pipes. *Water Res.* **2001**, *35* (14), 3283-3290, DOI: 10.1016/S0043-1354(01)00054-9.

[7] Beardsley, M.; Adams, C. D., Modeling and Control of Vinyl Chloride in Drinking Water Distribution Systems. *Environ. Eng.* **2003**, *129* (9), 844-851, DOI: 10.1061/(ASCE)0733-9372(2003)129:9(844).

[8] Dreher, E. L.; Torkelson, T. R.; Beutel, K. K., Ullmann's Encycl. *Ind. Chem. Chlorethanes Chloroethylenes.* **2011**, 748-750. DOI: 10.1002/14356007.o06_o01.

[9] Hunziker, H.; Kneppe, H.; McLean, A.; Siegbahn, P.; Wendt, H., Visible electronic absorption spectrum of vinyl radical. *Can. J. Chem.* **1983**, *61* (5), 993-995, DOI: 10.1139/v83-175.

[10] Drougas, E., Papayannis, D.K., Kosmas, A.M. Quantum Mechanical and Kinetic Studies of the Reaction of Methyl Radicals with Chlorine Molecules. *J. Phys. Chem. A.* **2002**, *106* (26), 6339-6345, DOI: 10.1021/ jp013094n.

[11] Timonen, R. S., Russell, J. J., Sarzynski, D.; Gutman, D., Kinetics of the reactions of unsaturated hydrocarbon free radicals (vinyl, allyl, and propargyl) with molecular chlorine. *J. Phys. Chem.* **1987**, *91* (7), 1873-1877, DOI: 10.1021/j100291a037.

[12] Lee, J.; Bozzelli, J. W.; Sawerysyn, J. P., *ab initio* calculations and thermochemical analysis on C1 atom abstractions of chlorine from chlorocarbons and the reverse alkyl abstractions: $Cl_2 + R\cdot \leftrightarrow Cl\cdot + RCl$. *Int. J. Chem. Kinet* **2000**, *32* (9), 548-565, DOI: 10.1002/1097-4601(2000)32:9<548::AID-KIN5>3.0.CO;2-P.

[13] Huang, J.; Li, X.; Zeng, G.; Cheng, X.; Tong, H.; Wang, D., Thermal decomposition mechanisms of poly(vinyl chloride): A computational study. *J. Waste Manag*. **2018**, *76*, 483-496. DOI: 10.1016/ j.wasman.2018.03.033.

[14] Mousavipour, S. H.; Asemani, S. S., Theoretical Study on the Dynamics of the Reaction of HNO(1A′) with HO_2(2A″), *J. Phys. Chem. A* **2015**, *119*, 5553-5565, DOI: 10.1021/acs.jpca.5b02838.

[15] Montgomery, J. A. Jr; Frisch, M. J.; Ochterski, J. W.; Petersson, G. A., A Complete Basis Set Model Chemistry. VI. Use of Density Functional Geometries and Frequencies. *J. Phys. Chem.* **1999**, *110* (6), 2822-2827. DOI: 10.1063/1.477924.

[16] Sylvetsky, N.; Peterson, K. A.; Karton, A.; Martin, J. M. L., Toward a W4-F12 Approach: Can Explicitly

Correlated and Orbital-Based Ab Initio CCSD(T) Limits be Reconciled? *J. Chem. Phys.* **2016**, *144*, 214101, DOI: 10.1063/1.4952410.

[17] Baer, T.; Hase, W. L., Unimolecular reaction dynamics: theory and experiments. Vol. 31. Oxford University Press on Demand. **1996**.

[18] Borjesson, L. E. B.; Nordholm, S., Microcanonical correlation analysis of collisional energy transfer efficient in unimolecular reaction, *J. Phys. Chem.* **1995**, *99* (3), 938-944, DOI: 10.1021/j100003a016.

[19] Loukhovitski, B. L.; Sharipov, A. S., Molecular Collision Diameters and Electronic Polarizabilities: Inherent Relationship and Fast Evaluation. *J. Phys. Chem. A*, **2021**, *125*, 5117-5123, DOI: 10.1021/ acs.jpca.1c02201

[20] Georgievskii, Y.; Klippenstein, S. J., Long-Range Transition State Theory. *J. Phys. Chem.* **2005**, *122* (19), 194103, DOI: 10.1063/1.1899603.

[21] Chesnavich, W. J.; Bowers, M. T., Statistical Phase Space Theory of Polyatomic Systems: Rigorous Energy and Angular Momentum Conservation in Reactions Involving Symmetric Polyatomic Species. *J. Phys. Chem. A.* **1977**, *66* (6), 2306-2315. DOI: 10.1063/ 1.434292.

[22] Saheb, V.; Rezaei, F.; Hosseini, S. M. A., DFT and Theoretical Kinetics Studies on the Reaction of Nitrate Radical with α-pinene and β-pinene. *Comput. Theor. Chem.* **2015**, *1051*, 123-128, DOI: 10.1016/ j.comptc.2014.10.027.

[23] Zhu, L.; Hase, W. L., A general RRKM program (QCPE 644), Quantum chemistry program exchange. Chemistry Department, University of Indiana, Bloomington, **1993**.

[24] Dean, A. M., Predictions of Pressure and Temperature Effects upon Radical Addition and Recombination Reactions. *J. Phys. Chem.* **1985**, *89* (21), 4600-4608, DOI: 10.1021/j100267a038.

[25] Brown, R. L. A Method of Calculating Tunneling Corrections For Eckart Potential Barriers. *J. Res. Natl. Bur. Stand. (U.S.)* **1981**, *86* (4), 357, DOI: 10.6028/jres.086.014.

[26] Eckart, C. The Penetration of a Potential Barrier by Electrons. *Phys. Rev.* **1930**, *35* (11), 1303, DOI: 10.1103/PhysRev.35.1303.

[27] Mousavipour, S. H.; Saheb, V.; Pirhadi, F.; Dehbozorgi, M. R., Experimental and Theoretical Study on the Kinetics and Mechanism of Thermal Decomposition of 1,2-Dichloroethane, *J. Iran. Chem. Soc.* **2007**, *4* (3), 279-298, DOI: 10.1007/BF03245977.

[28] Mousavipour, S. H.; Yousefiasl, I., Quasi-Classical Trajectory Dynamics Study on the Reaction of H with HO_2 Bull. *Chem. Soc. Jpn.*, **2009**, *82* (8), 953-962, DOI: 10.1246/bcsj.82.953.

[29] Yoder, L. M.; Barker, J. R., Quasi-classical Trajectory Simulations of Pyrazine-Argon and Methylpyrazine-Argon van der Waals Cluster Pre-dissociation and Collisional Energy Transfer, *J. Phys. Chem. A,* **2000**, *104* (45), 10184-10193, DOI: 10.1021/jp001248d.